FutureWater

Technical documentation

SPHY modelling for Roadside Spring Protection (ROSPRO)



CLIENT **Partners for Water**

AUTHORS **Tijmen Schults**

DATE **June 2025**

SPHY modelling for Roadside Spring Protection (ROSPRO)

Technical documentation

Client
Partners for Water

Authors
Tijmen Schults – Hydrologist and Remote Sensing Expert (t.schults@futurewater.nl)

Date
June 2025

FutureWater

ADDRESS
FutureWater B.V.
Costerweg 1V
6702 AA Wageningen
The Netherlands

TELEPHONE +31 317 460 050
WEBSITE www.futurewater.eu

Summary

This report documents the technical work conducted by FutureWater under the Roadside Spring Protection (RoSPro) project, with a focus on the development and application of a spatially explicit hydrological model (SPHY) and Decision Support System (DSS). The main objective was to simulate the impact of spring restoration interventions on groundwater recharge and spring discharge and to visualize the results in an accessible dashboard for decision-making. The work comprises model setup, calibration and validation, scenario simulations, spring discharge estimation and dashboard integration. The results inform scaling decisions by evaluating the hydrological effectiveness and feasibility of interventions, such as depression ponds and afforestation.

Content

Summary **3**

1 SPHY modelling **5**
1.1 Introduction 5
1.2 Model domain 5
1.3 Input data 6
1.4 SPHY spring module 7
1.4.1 Concept 7
1.4.2 Recharge area delineation 8
1.4.3 Travel time calculation 8
1.4.4 Groundwater losses 8
1.4.5 Spring discharge estimation 8
1.5 Calibration and validation 9
1.6 Scenario results 11

1 SPHY modelling

1.1 Introduction

The SPHY model for the ROSPRO project was developed to quantify the effects of landscape interventions on spring flows and regional water availability. This includes modelling spring hydrology at high spatial and temporal resolutions to compare intervention scenarios.

1.2 Model domain

The model domain includes the area around the Bhirgaun and Tankhuwa Streams, located in the Dhankuta and Chhathar Jorpati municipalities in eastern Nepal (Figure 1). These streams are fed by rainfall and springs. The colored dots in the image indicate the locations of the four springs where the interventions were implemented. The colored polygons show the recharge areas that contribute to the spring discharge. The springs in the area that are investigated are Chanchala Devi, Bojhey Khola, Keshari Kharka, and Dhoje Dharapaani. The selected springs are mostly located on the northern slopes at higher elevations within the basin.

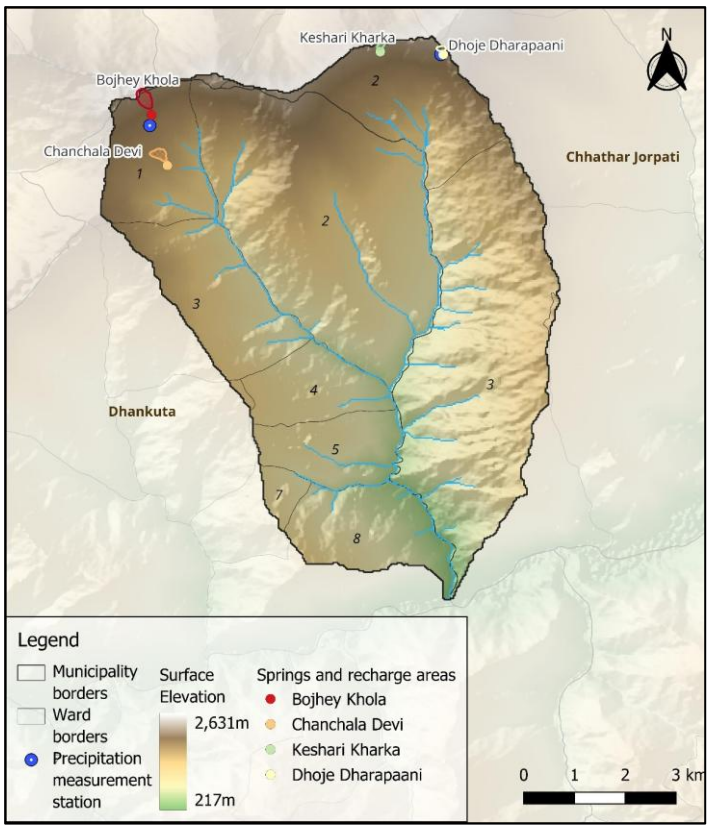


Figure 1. Model domain with the four spring locations.

A SPHY model was set up for this area of interest. The SPHY model simulated daily hydrological processes at a spatial resolution of 30 m from 2005 to 2024. The simulation covered the entire hydrological cycle, including snow, precipitation, evapotranspiration, infiltration, percolation, lateral flow, and base flow.

1.3 Input data

The SPHY model setup relies on multiple spatial and meteorological input datasets. Topography was defined using the Shuttle Radar Topography Mission (SRTM)[1] Digital Elevation Model (DEM). This DEM has a 30-meter resolution, serving as the base for hydrological flow routing. Meteorological forcing was provided by ERA5-Land Reanalysis[2] data, which included daily precipitation and minimum, maximum, and mean temperature. The temperature data were downscaled using lapse rate corrections to match the 30-meter grid resolution.

The land use map was derived from the ESA WorldCover 2021[3] product at 10-meter resolution. These classes were converted into crop coefficient (Kc) values for SPHY to estimate evapotranspiration across the landscape. Soil physical properties were retrieved from the HiHydroSoil dataset[4] (250-meter resolution) of FutureWater, which provided parameters like saturated hydraulic conductivity, field capacity, and wilting point, influencing infiltration, percolation, and groundwater recharge processes.

The rainfall data from the ERA5-Land dataset were validated using local station observations to assess their reliability for hydrological modelling in the study area (Figure 2). The comparison showed that ERA5-Land generally captured seasonal patterns well, particularly the monsoon-driven precipitation. However, a consistent overestimation of the total annual precipitation was observed. To correct for this bias, ERA5-Land precipitation data were adjusted using monthly correction factors derived from long-term station records and WorldClim[5] climatology. This improved the representation of both the magnitude and variability of precipitation, thereby enhancing the accuracy of the meteorological inputs of the model.

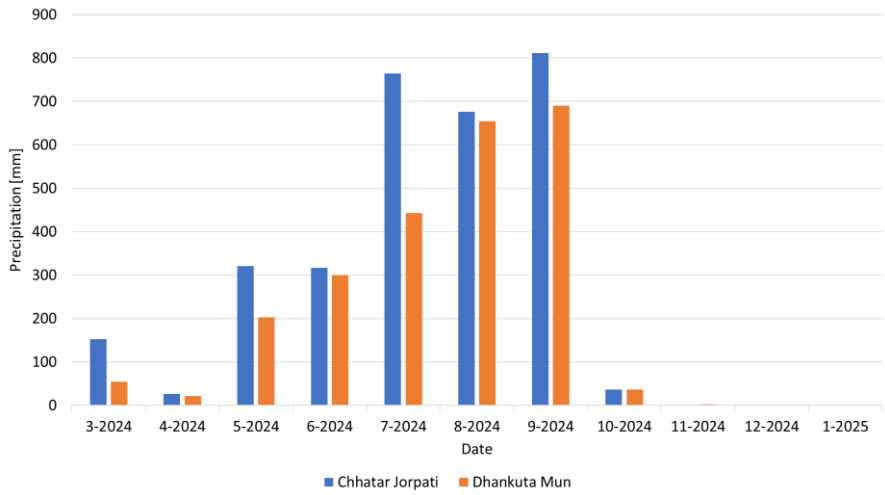


Figure 2. Monthly precipitation observations at Chhatar Jorpati and Dhankuta Mun.

[1] Farr, T. G., Rosen, P. A., Caro, E., Crippen, R., Duren, R., Hensley, S., ... & Alsdorf, D. (2007). *The Shuttle Radar Topography Mission*. Reviews of Geophysics, 45(2), RG2004. https://doi.org/10.1029/2005RG000183
[2] Muñoz-Sabater, J., Dutra, E., Agustí-Panareda, A., Albergel, C., Arduini, G., Balsamo, G., ... & Zsoter, E. (2021). *ERA5-Land: A state-of-the-art global reanalysis dataset for land applications*. Earth System Science Data, 13(9), 4349–4383. https://doi.org/10.5194/essd-13-4349-2021
[3] Zanaga, D., Van de Kerchove, R., De Keersmaecker, W., Sethi, G., Desclee, B., Achard, F., ... & Cartus, O. (2022). *ESA WorldCover 10 m 2021 v100*. Zenodo. https://doi.org/10.5281/zenodo.5571936

[4] Simons, G.W.H., R. Koster, P. Droogers. 2020. HiHydroSoil v2.0 - A high resolution soil map of global hydraulic properties. FutureWater Report 213.
[5] Fick, S. E., & Hijmans, R. J. (2017). *WorldClim 2: New 1-km spatial resolution climate surfaces for global land areas*. International Journal of Climatology, 37(12), 4302–4315. https://doi.org/10.1002/joc.5086

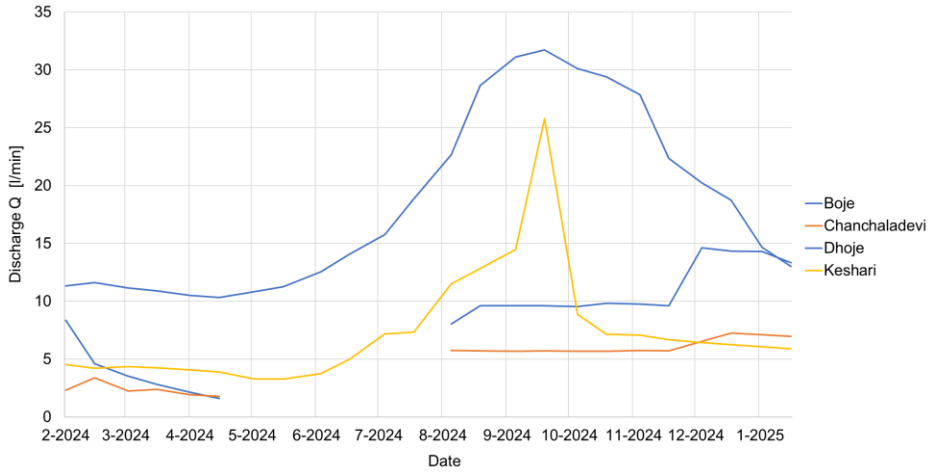


Figure 3. Spring discharge measured at the four selected springs.

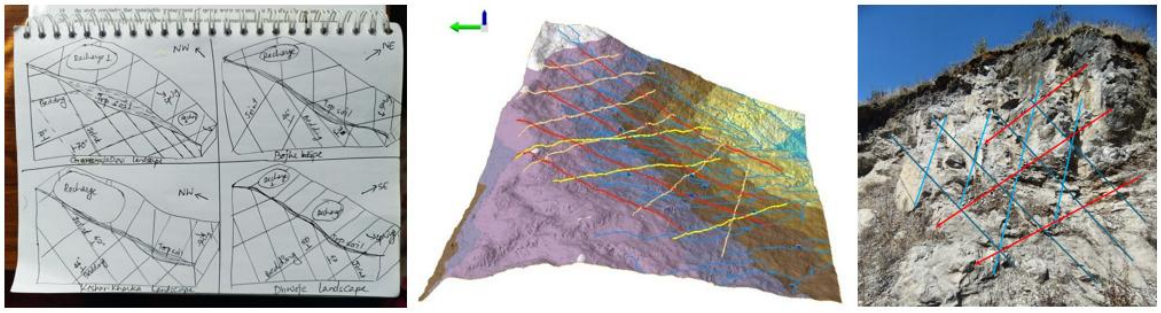


Figure 4. Detailed hydrogeological survey information.

1.4 SPHY spring module

1.4.1 Concept

The standard SPHY model simulates groundwater recharge at each time step for every pixel in the basin. However, the original SPHY model cannot simulate springs. Therefore, a dedicated SPHY spring module was developed to simulate spring discharge. The SPHY spring module translates spatially distributed groundwater recharge into time-delayed spring discharge using delineated spring recharge areas, hydrogeology, and observed discharge patterns. This approach allowed the model to simulate the lag between rainfall and spring response, as observed in the field, accounting for subsurface travel time and water losses during transit.

1.4.2 Recharge area delineation

Recharge areas for each spring were delineated through a hydrogeological survey early in the project. The polygons were converted into raster maps compatible with the SPHY model (.MAP format). These recharge areas represent zones where infiltrated water contributes to the target spring. The spring outlet locations were digitized and mapped, creating a spatial link between the recharge inputs and observed discharge points.

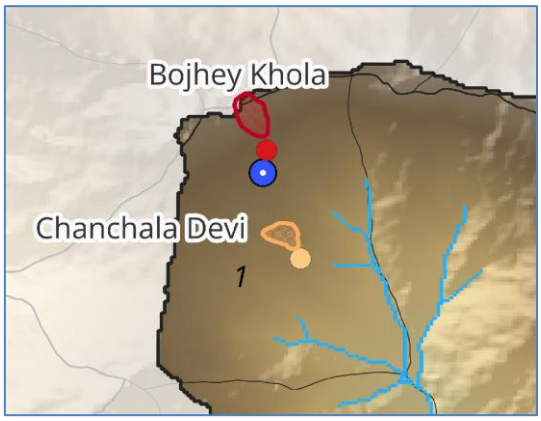


Figure 5. Springs and their recharge areas that contribute to spring discharge.

1.4.3 Travel time calculation

For each pixel in a spring's recharge area, the travel time (TT_{pixel}) was estimated. This represents the delay between groundwater recharge at a specific location and its contribution to the spring flow. TT was calculated using the 3-dimensional length of the flow path ($L_{flowpath}$) and hydraulic conductivity travel (K_{travel}) and adjusted based on the local hydrogeological setting.

$$TT_{pixel} = \frac{L_{flowpath}}{K_{travel}} \cdot (1 + cos(\theta)) \text{ [days]}$$

$L_{flowpath}$ = Flow path length [m], representing the distance groundwater travels to the spring
K_{travel} = Hydraulic conductivity for travel time [m/d]
θ = Tilt/angle of fracture/bedding plane in flow direction [°]

1.4.4 Groundwater losses

Not all recharged groundwater reaches springs. The hydrogeological setting of the study area is highly fractured, with faults in multiple directions. Consequently, a portion is lost to deeper groundwater systems. This loss was represented by a groundwater loss coefficient calibrated using the observed spring discharge data. The magnitude of the losses depended on the travel time and site-specific subsurface characteristics and was calibrated per spring to match the observed trends. Groundwater loss (D_{loss}) was calculated as follows:

$$D_{loss}(t) = K_{loss} \cdot R_{gw}(t)^{\tau} \text{ [mm]}$$

$D_{loss}(t)$ = Deep groundwater loss at timestep t [mm]
K_{loss} = Hydraulic conductivity for losses to deep groundwater [mm/d]
$R_{gw}(t)$ = Groundwater recharge at timestep t [mm]
τ = Groundwater diffusivity exponent [-]

1.4.5 Spring discharge estimation

Spring discharge was calculated at each time step by summing the delayed groundwater recharge contributions from all pixels in the recharge area after subtracting losses from deeper groundwater. A constant baseflow was added to each spring to correct the spring discharge for deeper groundwater additions that could not be explained by rainfall. This approach makes the model sensitive to both the

spatial structure of the recharge and the temporal dynamics of the spring system. The general formulation is as follows:

$$Q_{spring}(t) = \sum_{pixels}[R_{gw} - D_{loss}](t - TT) + Q_{bf}$$

Where:

$Q_{spring}(t)$	= Spring discharge at timestep t [mm]
$R_{gw}(t - TT)$	= Groundwater recharge at delayed timestep t – TT [mm]
$D_{\text{loss}}(t - TT)$	= Loss of water to deeper groundwater system at delayed timestep t – TT [mm]
TT	= Travel time from each pixel in the recharge area to the spring [days]
Q_{bf}	= Constant baseflow [l/m]

1.5 Calibration and validation

The calibration of the spring module was done by comparing simulated spring discharge against observed values for four target springs: Chanchala Devi, Dhwoje, Bohje, and Kesharikarka. The main objective was to reproduce the timing, amplitude, and seasonal dynamics of the observed discharge, with a particular focus on capturing the monsoon-driven peaks and the baseflow characteristics.

Each spring was assigned a unique set of hydrogeological parameters based on local geology, discharge behavior, and spatial configuration of the recharge areas. The hydrogeological parameters were iteratively selected by minimizing the RMSE between observations and simulated discharge and maximizing the R^2. The key parameters calibrated were as follows:

- K_{travel} [m/d]: effective horizontal hydraulic conductivity controlling the speed of groundwater flow from the recharge pixels to the spring.
- K_{loss} [m/d]: vertical conductivity capturing losses to deeper groundwater layers during transit
- TT [months] Travel time is derived from the flow path length and conductivity, which dictates the lag between recharge and discharge.
- Q_{bf} [l/min]: Constant baseflow estimated dry season discharge used for baseline comparisons.

Table 1. Calibrated hydrogeological parameters.

Spring	K_travel [m/d]	K_loss [m/d]	Baseflow [l/m]	Travel time [months]	R^2
Chanchala Devi	12	0.99	2	1.5	0.68
Dhwoje	8	0.91	11	1.8	0.92
Bohje	4	0.85	1	1.9	0.58
Kesharikarka	4	0.65	4	1.9	0.44

It can be seen that the calibrated hydrogeological parameters produce acceptable to good R^2 values for each spring. In particular, Dhwoje showed a good fit, capturing the seasonality of the monsoon and baseflow well (Figure 7). The full simulation with calibrated parameters for Dhwoje showed the interannual and intra-annual variability of spring discharge in the study area (Figure 8).

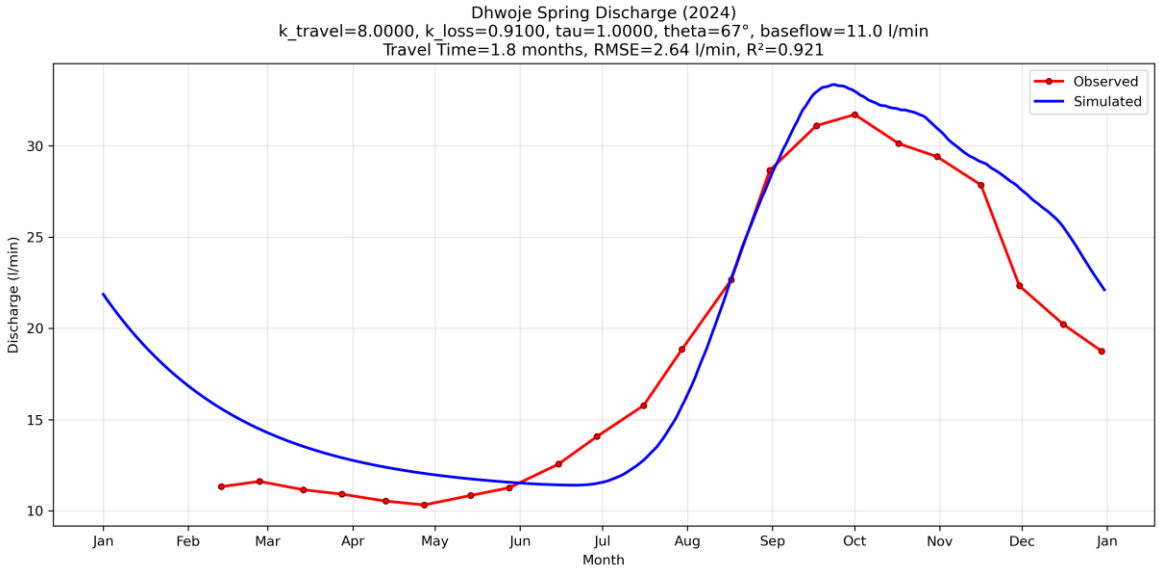


Figure 7. Observed and simulated discharge for Dhwoje spring in 2024.

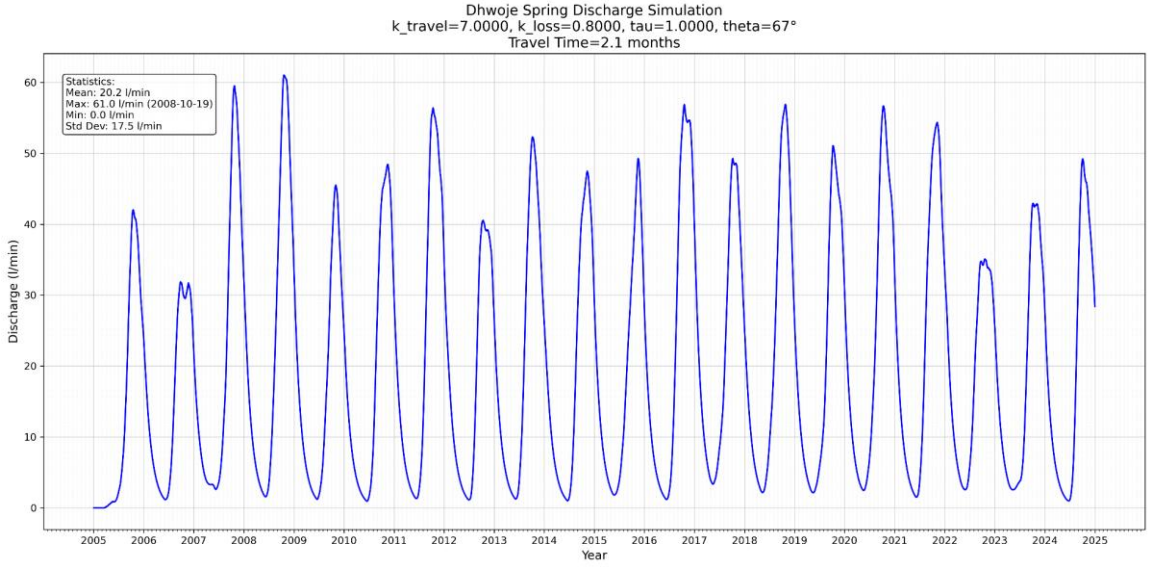


Figure 8. Full simulation of spring discharge for Dhwoje.

1.6 Scenario results

To evaluate the hydrological impact of the restoration measures, three intervention scenarios were developed and implemented in the SPHY model.

(i) **Baseline**: business-as-usual scenario.
(ii) **Pondings**: depression pond scenarios that enhance infiltration and groundwater recharge. [Soil depth * 0.8]
(iii) **Luchange**: A land-use change scenario with reduced vegetation (transpiration). [Kc * 0.8]

For each scenario, key model parameters, such as the saturated hydraulic conductivity, infiltration capacity, and crop coefficients (Kc), were adjusted accordingly. The spring module allowed the effects of these interventions on discharge dynamics to be assessed in terms of both the quantity and timing of spring flow, offering a basis for cost-benefit comparisons and upscaling potential.

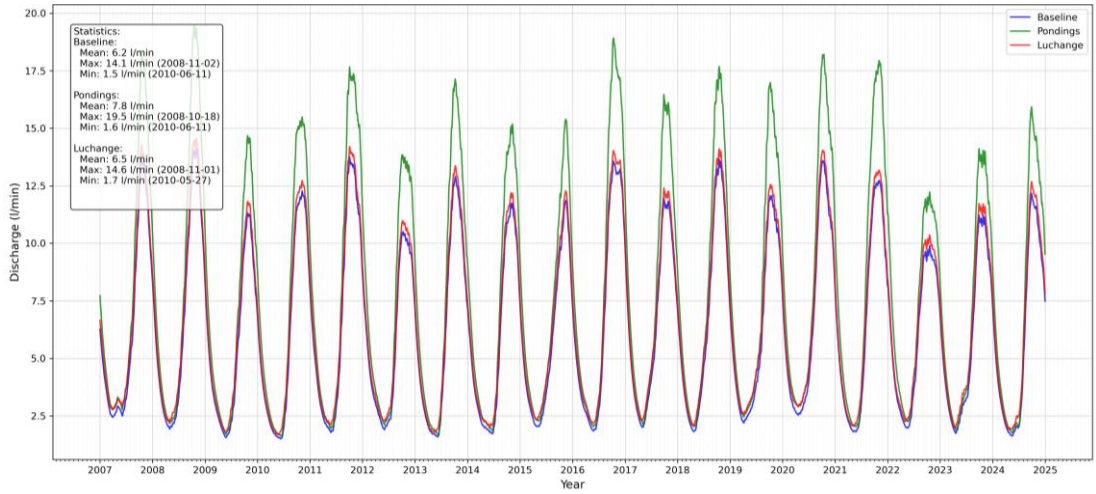


Figure 9. Bohje spring discharge full time series scenario comparison.

The plot shows the simulated spring discharge for the Bohje Spring over the period 2007–2024, comparing three different scenarios: Baseline, Pondings, and Luchange. The key observations from the results were as follows: seasonal patterns were visible, with peak discharges occurring consistently around the same period each year, driven by the monsoons. All scenarios followed a similar temporal pattern but differed in magnitude.

The ponding scenario showed a modest increase in discharge relative to the baseline. The average discharge increased from 6.2 l/min (baseline) to 7.8 l/min, with a peak of 19.5 l/min in October 2008, suggesting that depression ponds help retain and slowly release water to the spring. The land use change scenario had a lesser effect, with a mean discharge of 6.5 l/min, but significantly lower peaks than pondings (up to 14.6 l/min), but an overall higher year-round discharge than the baseline. This indicates that land-use changes could indicate a constant change in the baseflow contributions.

The minimum discharge values remained relatively close across the scenarios, but the land use change scenario showed a slightly elevated dry-season baseflow, implying better groundwater recharge and retention. In summary, the simulation suggests that both ponding structures and land use change improve spring discharge, with land use change having the strongest impact on enhancing and sustaining the flow, whereas ponding significantly increases capture and release in wet periods.

The results of this modelling exercise are used in the cost-benefit calculator and visualised in the decision-support system presented in the next chapter.